Bioorganic & Medicinal Chemistry Letters 23 (2013) 5300–5306

Contents lists available at ScienceDirect

Bioorganic & Medicinal Chemistry Letters

journal homepage: www.elsevier.com/locate/bmcl

Discovery of cyclic sulfoxide hydroxyethylamines as potent and selective β-site APP-cleaving enzyme 1 (BACE1) inhibitors: Structure based design and in vivo reduction of amyloid β-peptides

Heinrich Rueeger [a,*], Rainer Lueoend [a], Rainer Machauer [a], Siem Jacob Veenstra [a], Laura Helen Jacobson [b,†], Matthias Staufenbiel [b], Sandrine Desrayaud [c], Jean-Michel Rondeau [d], Henrik Möbitz [a], Ulf Neumann [b]

[a] Department of Global Discovery Chemistry, Institutes for BioMedical Research, Novartis Pharma AG, CH-4057 Basel, Switzerland
[b] Department of Neuroscience, Institutes for BioMedical Research, Novartis Pharma AG, CH-4057 Basel, Switzerland
[c] Metabolism and Pharmacokinetics, Institutes for BioMedical Research, Novartis Pharma AG, CH-4057 Basel, Switzerland
[d] Structural Biology Platform, Institutes for BioMedical Research, Novartis Pharma AG, CH-4057 Basel, Switzerland

ARTICLE INFO

Article history:
Received 14 June 2013
Revised 27 July 2013
Accepted 30 July 2013
Available online 9 August 2013

Keywords:
BACE-1
Inhibitor
Alzheimer's disease
Structure based design
Cyclic sulfoxide hydroxyethylamine
inhibitors
In vivo reduction of amyloid β-peptides

ABSTRACT

Previous structure based optimization in our laboratories led to the identification of a novel, high-affinity cyclic sulfone hydroxyethylamine-derived inhibitor such as **1** that lowers CNS-derived Aβ following oral administration to transgenic APP51/16 mice. Herein we report SAR development in the S3 and S2′ subsites of BACE1 for cyclic sulfoxide hydroxyethyl amine inhibitors, the synthetic approaches employed in this effort, and in vivo data for optimized compound such as **11d**.

Alzheimer's disease (AD) is one of the most prevalent neurodegenerative disorders among the elderly worldwide. Considerable evidence has accumulated indicating a central role of the amyloid-β (Aβ) peptide and specifically its aggregation in the pathogenesis of AD.[1] The pathway generating Aβ is initiated by BACE1, a membrane-bound aspartic protease (EC 3.4.23.46), cleaving the transmembrane protein β-amyloid precursor protein (APP).[2–6] The main products generated are the secreted amino-terminal part of APP (sAPPβ) and the carboxy-terminal fragment C99, which is further cleaved by γ-secretase leading to Aβ.[7,8] Knocking out the BACE1 gene not only blocks the generation of Aβ but also of C99 for which toxicity has been shown as well.[9–14] Knock out of BACE1 leads to hypomyelinization during development but not to general toxicity.[15–17] The inhibition of BACE1, therefore, is an attractive approach for the development of causal AD therapies.

We have previously described the design and synthesis of cyclic sulfone HEA (cHEA) BACE1 inhibitors exemplified by **1**, a high affinity inhibitor which demonstrated Aβ reduction in APP51/16 transgenic mice (Fig. 1).[18] In this Letter, we report our efforts to further optimize the cellular activity and thereby reduce CNS-derived Aβ at a lower oral dose (<100 μmol/kg). We hypothesized that the loss in potency observed between the enzymatic and

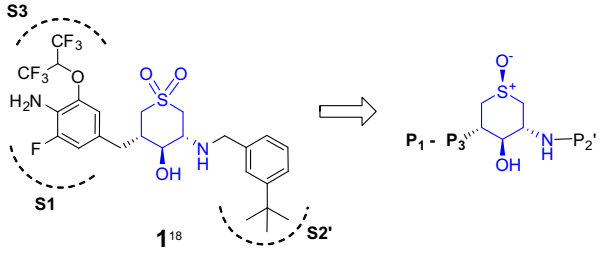

pKa	5.4
BACE1 IC_{50}	2 nM
CHO APPwt cell IC_{50}	55 nM
Papp in MDCK cells	40 nm/s
MDCK efflux ratio (ER)	4

Figure 1. In vitro profile of sulfone cHEA inhibitor **1**.

* Corresponding author. Tel.: +41 61 6963255; fax: +41 61 6962455.
E-mail address: heinrich.rueeger@novartis.com (H. Rueeger).
† Current affiliation: The Florey Institute of Neuroscience and Mental Health, University of Melbourne, Parkville 3010, Australia.

0960-894X/$ - see front matter © 2013 Elsevier Ltd. All rights reserved.
http://dx.doi.org/10.1016/j.bmcl.2013.07.071

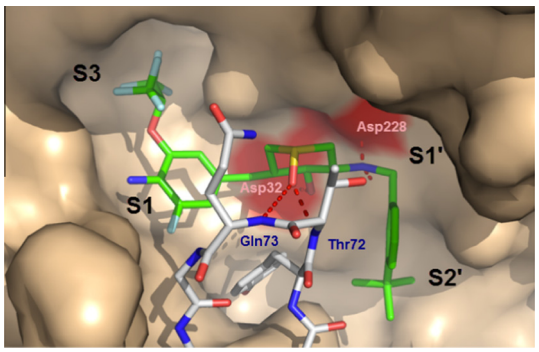

Figure 2. Cocrystal structure of **11a** (green) bound to BACE1.

cellular activity (up to 25-fold) in the sulfone containing cHEA inhibitor series was due to the low pK_a.[18] Therefore, our strategy for increasing the cellular activity was to raise the pK_a from 5.4 to >6.5 by replacing the sulfone with a sulfoxide moiety in the cHEA transition state mimetic (Fig. 1).[19] Retaining the key H-bond to Thr72 and Gln73 of the flap with an axially substituted sulfoxide (Fig. 2) was expected to provide an equipotent cHEA mimetic with potentially better pharmacokinetic properties due to the reduced number of heteroatoms.

The synthesis of the sulfoxide cHEA inhibitors as shown in Tables 1 and 2 is summarized in Scheme 1. The enantiopure intermediate **2**, previously synthesized in larger amounts for the preparation of sulfone containing cHEA inhibitors,[18] was initially extended with the P2′ fragment to allow the introduction of differ-

Table 1
Comparison of enzymatic and cellular activity of sulfone and sulfoxide cHEA inhibitors

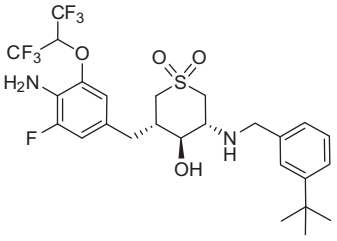

1

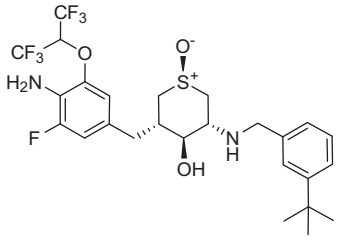

11a

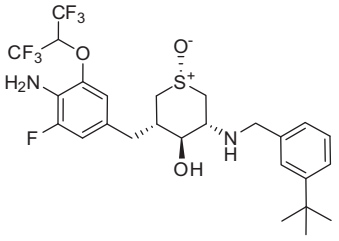

12a

Compd	IC_{50}[a] (μM)			Potency	P_{app}[c] (nm/s)	ER[d]	Log*P*	pK_a[e]
	hBACE1	CHO-APPwt cells	hCatD	Ratio[b]	MDCK			
1	0.002	0.055	0.45	22×	40	4	5.1	5.7
11a	0.002	0.014	0.87	7×	180	11	5.2	6.7
12a	0.088	0.330	>10	4×	110	13	4.9	n.d.

[a] Values are means of at least three experiments.
[b] The potency ratio measures the drop in potency observed in the cell-based assay relative to the enzyme-based assay.
[c] P_{app} is the permeability through a MDR1-MDCK cell monolayer transfected with human MDR1.
[d] ER is the efflux ratio ($P_{BL\text{-}AP}/P_{AP\text{-}BL}$) in MDCK cells transfected with human MDR1.
[e] pK_a measured with a Profiler SGA instrument using multi-wavelength UV spectroscopy and a linear 2–12 pH unit gradient.

Table 2
P3 SAR of sulfoxide cHEA inhibitors

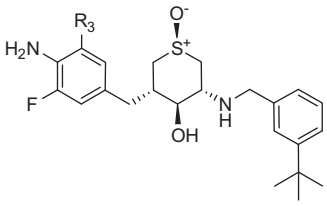

Compd	R^3	IC_{50}[a] (μM)			Potency	P_{app}[c] (nm/s)	ER[d]	Log*P*	IC_{50} (μM)
		hBACE1	CHO-APPwt cells	hCatD	Ratio[b]	MDCK			CYP3A4
11b	OCH_3	0.033	0.026	1.24	1	220	12	3.5	0.3
11c	OCH_2CF_3	0.008	0.062	1.20	8	190	16	4.3	0.3
11d	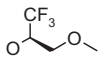	0.004	0.010	0.82	3	180	9	3.9	0.2
11f	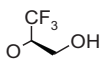	0.007	0.021	2.45	3	160	86	3.7	0.9
20	OH	0.530	1.34	1.78	3	90	27	n.d.	>10

[a] Values are means of at least three experiments.
[b] The potency ratio measures the drop in potency observed in the cell-based assay relative to the enzyme-based assay.
[c] P_{app} is the permeability through a MDR1-MDCK cell monolayer transfected with human MDR1.
[d] ER is the efflux ratio ($P_{BL\text{-}AP}/P_{AP\text{-}BL}$) in MDCK cells transfected with human MDR1.

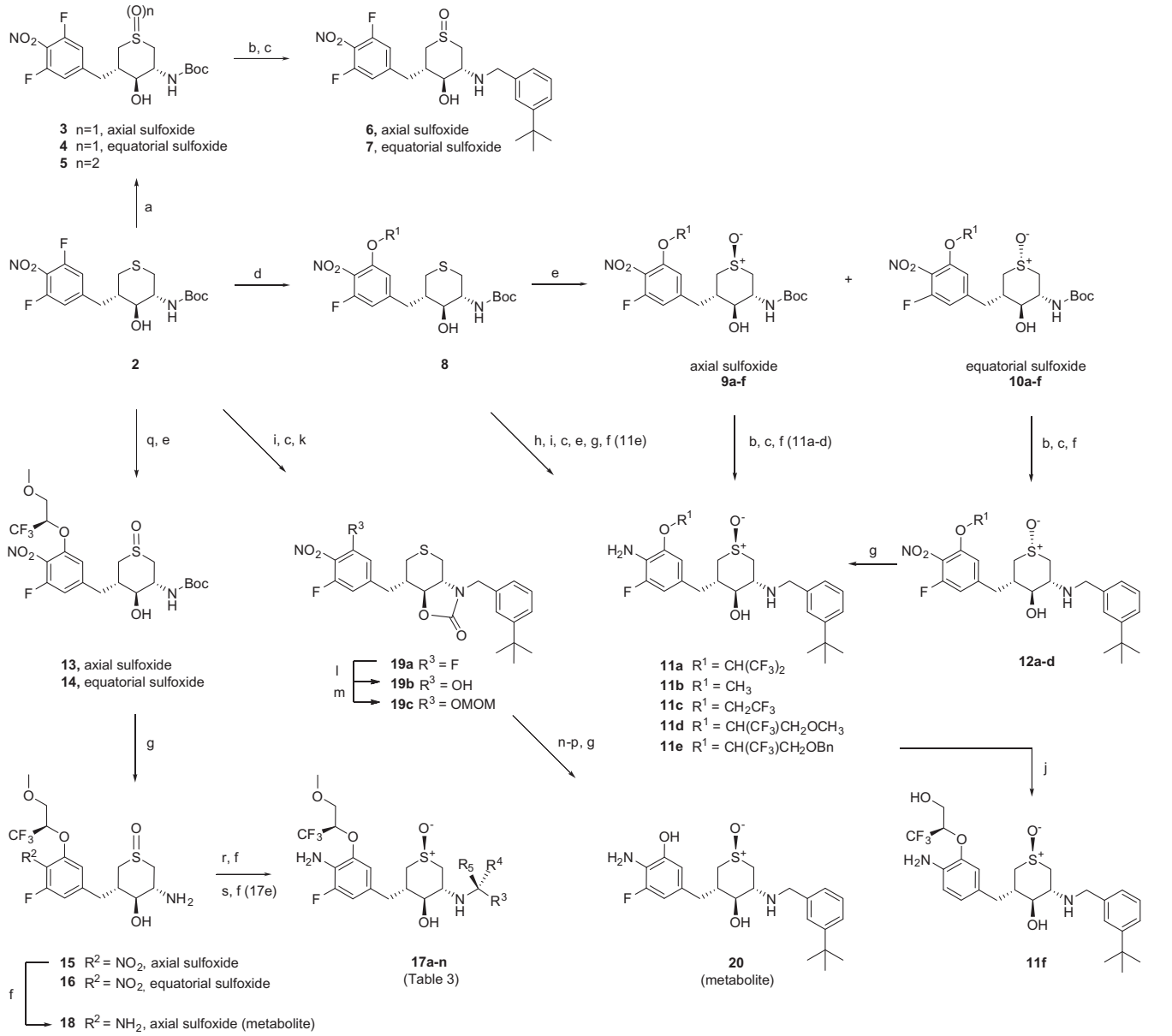

Scheme 1. Reagents and conditions: (a) potassium peroxymonosulfate, THF/H_2O (2:1), 25 °C; (b) TFA, CH_2Cl_2,1 h, 25 °C, 99%; (c) (1) 3-*tert*-butyl-benzaldehyde, NaOAc, CH_2Cl_2/MeOH (2:1), 2 h, 25 °C, (2) $NaBH_3CN$, MeOH, 1 h, 25 °C, 95%; (d) R-OH, KHMDS, THF, 24 h, 25 °C, 90–95%; (e) H_2O_2, AcOH/THF (1:3), 6 h, 25 °C, 96% or H_2O_2, 0.02 equiv $HAuCl_4$, MeOH, 5 h, 25 °C, 97%; (f) H_2, 10% Pd–C, MeOH, 4–6 h, 45 °C, 85–90%; (g) 3 N HCl in MeOH, 24 h, 25 °C, 95%; (h) (*R*)-3-benzyloxy-1,1,1-trifluoro-propan-2-ol, KO*t*Bu, THF, 0 °C, 82%; (i) 4 N HCl in dioxane, 25 °C, 99%; (j) BCl_3, CH_2Cl_2, −78 °C, 83%; (k) carbonyldiimidazole, NEt_3, cat. DMAP, acetonitrile, 2 h, 25 °C, 95%; (l) NaH, $CH_3SO_2(CH_2)_2OH$, DMF, 1.5 h, 25 °C, 95%; (m) MOM-Cl, *i*-Pr_2NEt, CH_2Cl_2, 0.5 h, 96%; (n) $NaIO_4$, THF/H_2O (2:1), 6 days, 25 °C, 74%; (o) H_2, 10% Pd–C, MeOH, 2.5 h, 45 °C, 92%; (p) KOTMS, THF, 1 h, 70 °C, 84%; (q) (*R*)-1,1,1-trifluoro-3-methoxypropan-2-ol, KOH, THF, 24 h, 40 °C, 92%; (r) (1) R-CHO, NaOAc, CH_2Cl_2/MeOH (2:1), 2 h, 25 °C, (2) $NaBH_3CN$, MeOH, 1 h, 25 °C, 80–95%; (s) (1) 1-(3-(*tert*-butyl)phenyl)ethanone, 3-methyl-1-butanol, 1 day reflux, (2) $NaBH_3CN$, MeOH, 1 h, 25 °C, 34%.

ent P3 fragments late in the synthesis. A nearly chemo selective oxidation of **2** to a mixture of sulfoxides **3** and **4** was achieved by the slow addition of 1 equiv of potassium peroxomonosulfate in THF–H_2O at 0 °C to avoid over-oxidation to the sulfone **5** (<5%). *N*-Boc cleavage with trifluoroacetic acid (TFA) and subsequent reductive amination with 3-*tert*-butyl-benzaldehyde provided sulfoxides **6** and **7**. The 1:1 mixture of axial and equatorial sulfoxide isomers could not be separated by column chromatography at any stage. On the other hand, preceding P3 extension of **2** followed by the chemoselective oxidation of thioether **8** with H_2O_2 in AcOH–THF provided a 1:1 mixture of sulfoxide isomers **9** and **10** which could be separated by column chromatography. Various attempts to increase the amount of the axial sulfoxide isomer by changing the oxidant or using metal catalysis[20] were not very successful. Only the $HAuCl_4$ catalyzed oxidation with H_2O_2[21] in MeOH slightly favored the formation of the axial isomer (2:1 ratio). Removal of the *N*-Boc protecting group with TFA and prime side extension via reductive amination followed by catalytic reduction of the nitro group provided the axial and equatorial sulfoxide inhibitors **11a–d** and **12a–d**, respectively. The configurational assignment was confirmed by co-crystallization of **11a** (Fig. 2) and **12a** with BACE1. Later, we discovered during *N*-Boc deprotection of **14** with 3 N HCl in MeOH, that the equatorial isomer could be equilibrated into the thermodynamically more stable axial isomer[22] providing a 9:1 equilibrium mixture of **15** and **16** after 24 h stirring at ambient temperature. An even higher ratio of 20:1 to **11a–d** was obtained by equilibration of the final sulfoxide isomer **12a–d**. Reductive amination of **16** with different P3-aldehyde and ketone fragments

followed by catalytic reduction of the nitro group gave access to **17a–n**. The deuterated analogs **17b** and **17d** were prepared from the corresponding deuterated aldehyde and reduction of the intermediate imine with $NaBD_3CN$. The phenolic metabolite **20** was synthesized from **2** by intermediate protection of the amino-alcohol moiety as the oxazolone **19a** after prime side extension to allow the introduction of the phenolic moiety under strongly basic conditions with 2-(methyl sulfonyl) ethanol. For the oxidation of the thioether to the sulfoxide the phenol group in **19b** was first protected by a MOM-ether (**19c**). Reduction of the nitro group, cleavage of the oxazolone moiety with KOTMS and subsequent sulfoxide equilibration with 3 N HCl in MeOH with concomitant MOM-ether cleavage afforded the metabolite **20**.

A comparison of the enzymatic potency and the cellular activity of the initial hexafluoroisopropoxy substituted 4-amino-fluorobenzyl sulfone cHEA inhibitor **1** with the sulfoxide analogs (**11a** and **12a**, Table 1) demonstrated that the axial sulfoxide **11a** was as potent and selective over cathepsin D as the sulfone cHEA inhibitor. The equatorial analog **12a**, on the other hand, which is not able to form a H-bond interaction with the flap residue Thr-72 (Fig. 2), showed a 40-fold lower activity. As expected the sulfoxide cHEA containing inhibitor **11a** displayed a higher cellular activity compared to the sulfone cHEA analog **1** (7-fold vs 22-fold potency ratio), which can be explained by the higher pK_a (6.7 vs 5.7). Equally important was the increase in permeability to a P_{app} of 180 nm/s, being in the range commonly observed for central nervous system drugs (>150 nm/s),[23] albeit at the expense of an increased P-gp-efflux ratio (ER 4 → 11) in the MDR1-MDCK cell monolayer assay. The pharmacokinetic evaluation of **11a** in mice indicated significant brain penetration. However, only a modest bioavailability (14%) was observed due to high clearance (129 mL/min/kg) and high first-pass metabolism most likely facilitated by the high lipophilicity (Log*P* 5.2).

Previous SAR exploration of the S3 pocket in thesulfone cHEA series[18] revealed the important binding contributions of the CF_3 group by H-bonding as well as by nonbonding protein–fluorine interactions.[24] The same interactions could be observed in the co-crystal structure of the sulfoxide cHEA inhibitor **11d** in BACE1, the H-bonding to Thr232 (3.2 Å) and a deeply buried water (3.1 Å) and the beneficial short orthogonal C–F contact to the amide of Gln12 (2.8 Å) (Fig. 3). The two CF_3 groups in the P3 fragment of **11a** were initially introduced to completely abolish the formation of the phenolic metabolite **20**. Removal of one of the CF_3 groups provided the less lipophilic compound **11c** (Log*P* 4.3) with much higher plasma and brain levels in APP51/16 transgenic mice (Table 4), however, with a fourfold lower potency in the enzymatic assay (IC_{50} = 8 nM). A possible explanation for the lower cellular activity of **11c** (IC_{50} = 62 nM, eightfold potency ratio) compared to the methoxy compound **11b** (IC_{50} = 26 nM) could be the higher lipophilicity (Log*P* 4.3 vs 3.5). The substitution of one of the CF_3 group of **11a** by a methoxymethyl ether provided the more polar compound **11d** (Log*P* 3.9) with more potent cellular activity (IC_{50} = 10 nM), a lower potency ratio (<threefold), good permeability (P_{app} 180 nm/s) and a slightly lower ER of 9. The more polar alcohol **11f** (Log*P* 3.7) exhibited a twofold lower potency in both assays, however, the presence of an additional H-bond donor resulted in a drastic increase in the ER (9 → 86). Overall, the insertion of more polar P3 fragments had only a minor effect on the undesired CYP3A4 interaction.

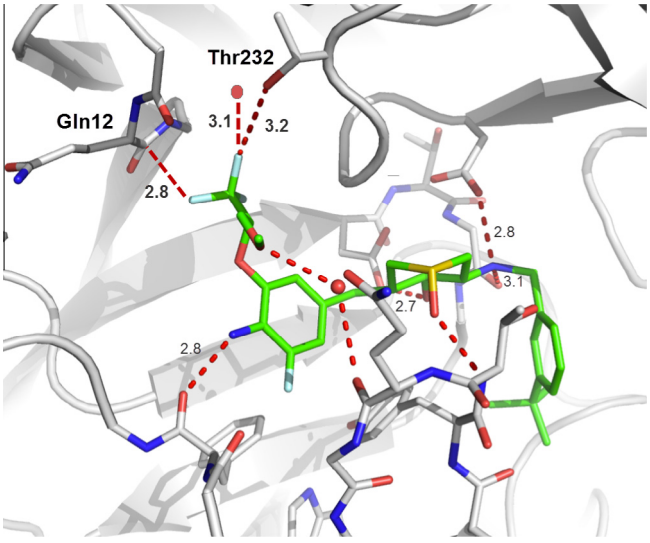

Figure 3. Cocrystal structure of **11d** (green) bound to BACE1.

In vitro metabolite identification studies of **11d** using liver microsomes suggested that oxidation at the *N*-benzylic tethered prime side fragment was the main site of metabolism as observed in other HEA inhibitors.[25] The different modifications of the prime-side fragment to improve the metabolic stability are summarized in Table 3. Since di-alkylation of the benzylic position was prohibited due to steric interference with the cHEA scaffold, the deuterated analogs **17b** and **17d** were prepared to gain some metabolic stability from the deuterium isotope effect.[26] Subsequent metabolic stability assessment in mouse and human liver microsomes showed only a minor improvement, indicating a 'masked' metabolic reaction in which the formation of the active oxygenating species had occurred prior to the isotopically sensitive C–H bond cleavage.[27] A few small steric modifications in the vicinity of the benzylic position were tolerated without considerable loss of potency, like the (*R*)-phenethylamine analog **17e** and the ortho–fluoro substituted analog **17g**, however, having no positive effect on the microsomal stability. Subsequently, we focused our attempts to improve the metabolic stability by reducing the lipophilicity of the P2′ fragment. As shown with several representative examples, the incorporation of polar functionalities (**17h–k**) or more polar heterocyclic ring systems (**17l–n**) led to a reduction of the CYP3A4 interaction and to an improvement of the metabolic stability in human (HLM) as well as mouse (MLM) liver microsomes. Unfortunately, this beneficial effect was associated with an at least threefold lower enzymatic and cellular activity and a higher ER (17–41). In comparison to the initial 3-*tert*-butyl-benzyl P2′ fragment of **11d**, no equipotent prime side fragment with improved in vitro metabolic stability could be identified.

In general, all compounds from this series displayed high systemic blood clearance. To assess the effect of BACE1 inhibition on brain $A\beta_{40}$ levels, compounds with the highest cellular activity (IC_{50} <50 nM), good permeation properties and a moderate ER (<15–20)[28] were tested in male or female human wild-type APP transgenic mice (APP51/16).[14,18,29] After oral administration exposure in blood and brain, as well as $A\beta_{40}$ forebrain concentrations were measured at 4 h post-dose.

The results of these experiments are shown in Table 4. The only moderate $A\beta_{40}$ reduction of **11a** despite high brain exposure can be explained with the very low unbound brain concentration (f_u <0.01) probably induced by the lipophilic $OCH(CF_3)_2$ P3 residue, which was introduced as a means to completely block the formation of the phenolic metabolite **20**.[30] The expected over-proportional increase of blood levels at higher oral doses, caused by saturation of the first-pass clearance, could be demonstrated with **11c** and **11d** in male mice. The most efficacious inhibitor **11d** lowered brain $A\beta_{40}$ levels by 62% at the highest dose of 180 μmol/kg and 39% at 100 μmol/kg (p <0.0001 vs vehicle treated group, 2-tailed Student's *t*-test). A slightly lower $A\beta_{40}$ reduction (38%) was achieved with **11c**, despite higher blood and brain exposure,

Table 3
P2′ SAR of sulfoxide cHEA inhibitors

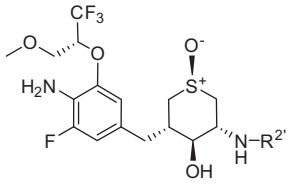

Compd	$R^{2'}$	IC_{50}[a] (μM)			P_{app}[b] (nm/s)	ER[c]	Log*P*	IC_{50} (μM)	HLM/MLM[d] (μL/min/mg)
		hBACE1	CHO-APPwt cells	hCatD	MDCK			CYP3A4	
18	H	150						>10	190/180
17a	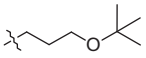	>10							
11d	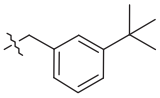	0.004	0.010	0.82	180	9	3.9	0.2	500/480
17b	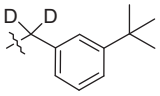	0.004	0.012	1.20	190	10	n.d.	0.1	600/530
17c	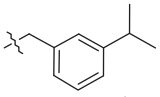	0.018	0.044	4.03	200	17	3.7	0.7	690/550
17d	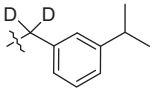	0.016	0.031	3.29	n.d.	n.d.	3.7	n.d.	600/660
17e	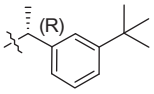	0.010	0.032	0.75	170	9		0.1	600/730
17g	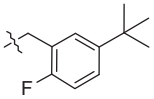	0.010	0.038	0.29	240	9	4.1	0.1	400/580
17h	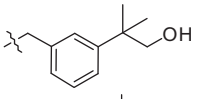	0.012	0.134	3.39	100	17	3.4	1.0	80/210
17i	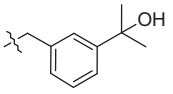	0.013	0.126	7.90	80	25		2.4	40/150
17j	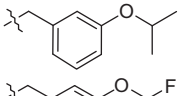	0.080	0.075	0.78	210	26	3.6	0.9	280/190
17k	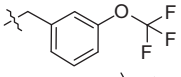	0.212	0.382	6.83	310	17	3.7	4.7	300/180
17l	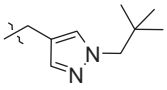	0.021	0.124	9.68	100	24	2.9	3.6	140/380
17m	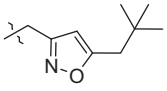	0.019	0.764[e]	3.57	190	41	3.1	1.1	580/510
17n	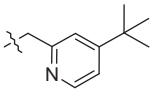	0.226	0.422	>10	190	26	3.5	1.6	140/400

[a] Values are means of at least three experiments.
[b] P_{app} is the permeability through a MDR1-MDCK cell monolayer transfected with human MDR1.
[c] ER is the efflux ratio ($P_{BL\text{-}AP}/P_{AP\text{-}BL}$) in MDCK cells transfected with human MDR1.
[d] Compounds were incubated with human (HML) or mouse (MLM) microsomes at 37 °C. The in vitro metabolic clearance rate was derived from data collected at four time points (0, 5, 15 and 30 min) in a reaction including cofactor(s) (NADPH and/or UDPGA).
[e] The low cellular activity of **17m** can be explained by the low pK_a of 4.9.

which can be explained with the threefold lower cellular activity. A significantly higher exposure and stronger pharmacodynamic response could not be observed with the deuterated *N*-benzyl analogs **17b** and **17d** in comparison to the non-deuterated analogs **11d** and **17c**, respectively. However, reduced levels of the amine metabolite **18** could be observed. For **17b** 37% versus 120% of

Table 4
PK-PD of 3-alkoxy substituted benzyl sulfoxide cHEA inhibitors

Compd	Dose (μmol/kg)	Gender[29]	Concd blood[a] (nmol/mL)	% of parent in blood		Concd brain[d] (nmol/g)	Rat brain f_u	Brain $A\beta_{40}$ reduction[e] (%), 4 h pd[f]
				18[b]	**20**[c]			
11a	180	Male	0.9	n.d.	<1	0.8	<0.01	32[g]
11c	180	Male	6.1	25	4	1.3	0.02	38[g] 27[g] 18[g]
	100	Male	2.6	40	4	0.7		
	60	Male	0.8	94	10	0.4		
11d	180	Male	3.8	38	25	0.7	0.02	62[g] 39[g] 23[h] 60[g] 39[g]
	100	Male	1.0	77	18	0.2		
	60	Male	0.3	120	23	0.1		
	60[j]	Female	5.2	4	<1	0.8		
	20[j]	Female	2.1	5	<1	0.5		
17b	60	Male	0.4	37	10	0.1	0.02	22[i]
17c	100	Female	1.6	22	n.d.	0.2	0.04	31[g]
17d	100	Female	1.5	12	n.d.	0.3		28[i]
17e	100	Female	5.4	10	n.d.	0.7	0.02	34[g]

[a] Concentrations in blood (nmol/mL = μM) obtained at 4 h after po application to APP51 transgenic mice. The oral formulation was a suspension in water containing 2% cremophor.
[b] Percent of amine metabolite **18** versus parent inhibitor formed in blood after 4 h.
[c] Percent of phenol metabolite **20** versus parent inhibitor formed in blood after 4 h.
[d] Concentrations in brain (nmol/g) obtained at 4 h after po application to APP51 transgenic mice.
[e] % mean reduction compared to the mean of the vehicle control.
[f] pd: post dose.
[g] $p \leqslant 0.0003$.
[h] $p = 0.02$.
[i] $p \leqslant 0.003$.
[j] Coadministration of Ritonavir (12.5 mg/kg) orally applied 0.5 h before administration of inhibitor.

parent **11d** at the dose of 60 μmol/kg and for **17d** 12% versus 22% of parent **17c** at a dose of 100 μmol/kg (Table 4), indicated a partial deuterium effect. The higher brain concentration of **17e** (0.7 nmol/g) achieved with the 100 μmol/kg dose compared to **11d** (0.2 nmol/g), both having the same brain f_u, did not translate into a higher $A\beta_{40}$ reduction (34% and 31%, respectively) at the 4 h time point.[31]

Having successfully demonstrated that potent sulfoxide cHEA inhibitors can significantly lower brain $A\beta_{40}$ levels, but fell short on achieving sufficient systemic drug exposure at lower doses, we investigated the pharmacokinetic boosting with sub-therapeutic doses of Ritonavir, to reduce the high clearance caused by CYP3A4 metabolism. The co-administration of the strong CYP3A4 inhibitor Ritonavir, also known as 'pharmaco enhancement', has been successfully employed in most marketed HIV inhibitors to reduce drug load.[32] Co-administration of Ritonavir (12.5 mg/kg po, 0.5 h prior to drug application) with the most efficacious inhibitor **11d** produced the same $A\beta_{40}$ reduction after 4 h (39%, p <0.0001) at the fivefold lower oral dose of 20 μmol/kg in APP51/16 transgenic mice. This considerable boosting effect was further substantiated by the >twofold higher plasma (2.1 nmol/mL) and brain levels (0.5 nmol/g) in comparison to the standard dose of 100 μmol/kg. In addition, the formation of the main amine metabolite **18** as well as the phenolic metabolite **20** were dramatically reduced (⩽5%, respectively, <1% of parent).

In conclusions, the replacement of the sulfone cHEA scaffold by the slightly more basic sulfoxide cHEA scaffold led to highly potent, selective inhibitors with improved cellular activity (**11d**, IC_{50} 10 nM). Sufficient CNS exposure could be achieved with a single oral dose of 60 μmol/kg to effect significant reduction in brain Aβ in APP51/16 transgenic mice. The high CYP3A4 mediated metabolic clearance inherent to this class of cHEA inhibitors could not be reduced to an acceptable level by chemical modifications. With the co-administration of the strong CYP3A4 inhibitor Ritonavir this liability could be minimized leading to a substantial exposure enhancement and subsequent brain $A\beta_{40}$ reduction at an acceptable oral dose of 20 μmol/kg. Detailed pharmacokinetic and pharmacodynamic studies in different species will be the subject of future communication.

Supplementary data

Supplementary data associated with this article can be found, in the online version, at http://dx.doi.org/10.1016/j.bmcl.2013.07.071.

References and notes

1. Citron, M. *Nat. Rev. Drug Disc.* **2010**, *9*, 387.
2. Hussain, I.; Powell, D.; Howlett, D. R.; Tew, D. G.; Meek, T. D.; Chapman, C.; Gloger, I. S.; Murphy, K. E.; Southan, C. D.; Ryan, D. M.; Smith, T. S.; Simmons, D. L.; Walsh, F. S.; Dingwall, C.; Christie, G. I. *Mol. Cell. Neurosci.* **1999**, *14*, 419.
3. Lin, X.; Koelsch, G.; Wu, S.; Downs, D.; Dashti, A.; Tang, J. *Proc. Natl. Acad. Sci. U.S.A.* **2000**, *97*, 1456.
4. Sinha, S.; Anderson, J. P.; Barbour, R.; Basi, G. S.; Caccavello, R.; Davis, D.; Doan, M.; Dovey, H. F.; Frigon, N.; Hong, J.; Jacobson-Croak, K.; Jewett, N.; Keim, P.; Knops, J.; Lieberburg, I.; Power, M.; Tan, H.; Tatsuno, G.; Tung, J.; Schenk, D.; Seubert, P.; Suomensaari, S. M.; Wang, S.; Walker, D.; Zhao, J.; McConlogue, L.; John, V. *Nature* **1999**, *402*, 537.
5. Vassar, R.; Bennett, B. D.; Babu-Khan, S.; Kahn, S.; Mendiaz, E. A.; Denis, P.; Teplow, D. B.; Ross, S.; Amarante, P.; Loeloff, R.; Luo, Y.; Fisher, S.; Fuller, J.; Edenson, S.; Lile, J.; Jarosinski, M. A.; Biere, A. L.; Curran, E.; Burgess, T.; Louis, J. C.; Collins, F.; Treanor, J.; Rogers, G.; Citron, M. *Science* **1999**, *286*, 735.
6. Yan, R.; Bienkowski, M. J.; Shuck, M. E.; Miao, H.; Tory, M. C.; Pauley, A. M.; Brashier, J. R.; Stratman, N. C.; Mathews, W. R.; Buhl, A. E.; Carter, D. B.; Tomasselli, A. G.; Parodi, L. A.; Heinrikson, R. L.; Gurney, M. E. *Nature* **1999**, *402*, 533.
7. Duff, K.; Eckman, C.; Zehr, C.; Yu, X.; Prada, C. M.; Perez-tur, J.; Hutton, M.; Buee, L.; Harigaya, Y.; Yager, D.; Morgan, D.; Gordon, M. N.; Holcomb, L.; Refolo, L.; Zenk, B.; Hardy, J.; Younkin, S. *Nature* **1996**, *383*, 710.
8. Scheuner, D.; Eckman, C.; Jensen, M.; Song, X.; Citron, M.; Suzuki, N.; Bird, T. D.; Hardy, J.; Hutton, M.; Kukull, W.; Larson, E.; Levy-Lahad, E.; Viitanen, M.; Peskind, E.; Poorkaj, P.; Schellenberg, G.; Tanzi, R.; Wasco, W.; Lannfelt, L.; Selkoe, D.; Younkin, S. *Nat. Med.* **1996**, *2*, 864.
9. Oster-Granite, M. L.; McPhie, D. L.; Greenan, J.; Neve, R. L. *J. Neurosci.* **1996**, *16*, 6732.
10. Cai, H.; Wang, Y.; McCarthy, D.; Wen, H.; Borchelt, D. R.; Price, D. L.; Wong, P. C. *Nat. Neurosci.* **2001**, *4*, 233.
11. Luo, Y.; Bolon, B.; Kahn, S.; Bennett, B. D.; Babu-Khan, S.; Denis, P.; Fan, W.; Kha, H.; Zhang, J.; Gong, Y.; Martin, L.; Louis, J. C.; Yan, Q.; Richards, W. G.; Citron, M.; Vassar, R. *Nat. Neurosci.* **2001**, *4*, 231.
12. Roberds, S. L.; Anderson, J.; Basi, G.; Bienkowski, M. J.; Branstetter, D. G.; Chen, K. S.; Freedman, S. B.; Frigon, N. L.; Games, D.; Hu, K.; Johnson-Wood, K.;

Kappenman, K. E.; Kawabe, T. T.; Kola, I.; Kuehn, R.; Lee, M.; Liu, W.; Motter, R.; Nichols, N. F.; Power, M.; Robertson, D. W.; Schenk, D.; Schoor, M.; Shopp, G. M.; Shuck, M. E.; Sinha, S.; Svensson, K. A.; Tatsuno, G.; Tintrup, H.; Wijsman, J.; Wright, S.; McConlogue, L. *Hum. Mol. Genet.* **2001**, *10*, 1317.
13. Dominguez, D.; Tournoy, J.; Hartmann, D.; Huth, T.; Cryns, K.; Deforce, S.; Serneels, L.; Camacho, I. E.; Marjaux, E.; Craessaerts, K.; Roebroek, A. J.; Schwake, M.; D'Hooge, R.; Bach, P.; Kalinke, U.; Moechars, D.; Alzheimer, C.; Reiss, K.; de Saftig, P.; Strooper, B. *J. Biol. Chem.* **2005**, *280*, 30797.
14. Rabe, S.; Reichwald, J.; de Ammaturo, D.; Strooper, B.; Saftig, P.; Neumann, U.; Staufenbiel, M. *J. Neurochem.* **2011**, *119*, 231.
15. Hu, X.; Hicks, C. W.; He, W.; Wong, P.; Macklin, W. B.; Trapp, B. D.; Yan, R. *Nat. Neurosci.* **2006**, *9*, 1520.
16. Sankaranarayanan, S.; Price, E. A.; Wu, G.; Crouthamel, M. C.; Shi, X. P.; Tugusheva, K.; Tyler, K. X.; Kahana, J.; Ellis, J.; Jin, L.; Steele, T.; Stachel, S.; Coburn, C.; Simon, A. J. J. *Pharmacol. Exp. Ther.* **2008**, *324*, 957.
17. Willem, M.; Garratt, A. N.; Novak, B.; Citron, M.; Kaufmann, S.; Rittger, A.; DeStrooper, B.; Saftig, P.; Birchmeier, C.; Haass, C. *Science* **2006**, *314*, 664.
18. Rueeger, H.; Lueoend, R.; Rogel, R.; Rondeau, J.-M.; Möbitz, H.; Machauer, R.; Jacobson, L.; Staufenbiel, M.; Desrayaud, S.; Neumann, U. *J. Med. Chem.* **2012**, *55*, 3364.
19. An estimate of the pK_a shift from a β-substituted sulfonyl amine to a sulfoxyl amines cannot be given since the data of corresponding analogs have not been documented. Calculation with Advanced Chemistry Development (ACD/Labs) Software V11.02 (© 1994–2012 ACD/Labs) predict a higher pK_a for the β-substituted sulfoxyl amine analogs.
20. (a) Zhao, H.; Samuel, O.; Kagan, H. B. *Tetrahedron* **1987**, *43*, 5135; (b) Legros, J.; Bolm, C. *Chem. Eur. J.* **2005**, *11*, 1086; (c) Yamaguchi, T.; Matsumoto, K.; Saito, B.; Katsuki, T. *Angew. Chem., Int. Ed.* **2007**, *46*, 4729; (d) O'Mahony, G. E.; Ford, A.; Maguire, A. R. *J. Org. Chem.* **2012**, *77*, 3288.
21. Yuan, Y.; Bian, Y. *Tetrahedron Lett.* **2007**, *48*, 8518.
22. (a) Johnson, C. R.; McCants, D. *J. Am. Chem. Soc.* **1964**, *86*, 2935; (b) Johnson, C. R.; McCants, D. *J. Am. Chem. Soc.* **1965**, *87*, 1109.
23. Mahar Doan, K. M.; Humphreys, J. E.; Webster, L. O.; Wring, S. A.; Shampine, L. J.; Serabjit-Singh, C. J.; Adkison, K. K.; Polli, J. W. *J. Pharmacol. Exp. Ther.* **2002**, *303*, 1029.
24. Dalvit, C.; Vulpetti, A. *ChemMedChem* **2011**, *6*, 104.
25. Charrier, N.; Clarke, B.; Cutler, L.; Demont, E.; Dingwall, C.; Dunsdon, R.; Hawkins, J.; Howes, C.; Hubbard, J.; Hussain, I.; Maile, G.; Matico, R.; Mosley, J.; Naylor, A.; O'Brien, A.; Redshaw, S.; Rowland, P.; Soleil, V.; Smith, K. J.; Sweitzer, S.; Theobald, P.; Vesey, D.; Walter, D. S.; Wayne, G. *Bioorg. Med. Chem. Lett.* **2009**, *19*, 3664.
26. Tung, R. *Innov. Pharm. Technol.* **2010**, *32*, 24.
27. (a) Fisher, M. B.; Henne, K. R.; Boer, J. *Curr. Opin. Drug Discovery Dev.* **2006**, *9*, 101; (b) Nelson, S. D.; Trager, W. F. **2003**, *Drug Metab. Dispos. 31*, 1481.
28. In our MDR1-MDCK cell monolayer assay, an ER of 10–20 was considered moderate and acceptable, since substantial brain exposure was observed with good permeating compounds (P_{app} >180 nm/s) and an ER of 15–20.
29. (a) Gandhi, M.; Aweeka, F.; Greenblatt, R. M.; Blaschke, T. F. *Annu. Rev. Pharmacol. Toxicol.* **2004**, *44*, 499; (b) Martignoni, M.; Groothuis, G. MM.; de Kanter, R. *Expert Opin. Drug Discovery* **2006**, *2*, 875.
30. The AMES test of the phenol **20** did not show any evidence of a mutagenic potential.
31. The observed exposure differences could also be explained by the gender difference of the individual animal groups.
32. (a) Moyle, G. L.; Back, D. *HIV Med.* **2001**, *2*, 105; (b) Boffito, M.; Maitland, D.; Samarasinghe, Y.; Pozniak, A. *Combinations Curr. Opin. Infect. Dis.* **2005**, *18*, 1.